Study of Moisture Transfer in Transverse Directions of Timber Members of Anhui Fir

Kongyang Chen[1], Menglin Sun[2] and Hongxing Qiu[1*]
[1]*Key laboratory of Concrete and Prestressed Concrete Structures of Ministry of Education, School of Civil Engineering, Southeast University, Nanjing, China*
[2]*Architecture Design Institute, China Railway Liuyuan Group Co. Ltd., Tianjin, China*

Keywords: Timber members, Moisture transfer, Diffusion coefficient, Surface emission coefficient, Finite element method.

Abstract: Anhui fir is a common building material in southeast China. As the basement of the research for shrinkage cracks and durability of timber structures in natural environment, this paper investigates the moisture content distribution and moisture transfer process in transverse cross-section of timber members made of Anhui fir. Now, the mostly used equations for calculating diffusion coefficient and surface emission are based on Norway spruce, which is actually not suitable for Anhui fir due to their different kinds of trees. Firstly, based on Fick's second law, the diffusion parameters and boundary conditions in humidity field and temperature field were analogized. Then, experiment in constant temperature and relative humidity was done. Experimental result showed the polynomial moisture content distribution in transverse direction, and exponential change with time, which was used for deriving new formulas for calculating diffusion coefficient and surface emission coefficient of Anhui fir. Finally, the Abaqus heat transfer analysis was used to simulate the moisture transfer process by substituting corresponding parameters successfully, and the results agreed well with experiment.

SCITEPRESS
SCIENCE AND TECHNOLOGY PUBLICATIONS

1 INTRODUCTION

Anhui fir is a common wood material used in Chinese timber structures, especially in southeast China. As an important building material, the physical and mechanical properties of wood are highly affected by its own moisture content (MC), including shrinkage/swelling, deformation, elastic modulus, and strength (Toratti, 1994, Ranta-Maunus, 2003, Hoyle Jr et al., 2007). Besides, wood is a hygroscopic material which absorbs or desorbs moisture to maintain equilibrium moisture content (EMC) corresponding to relative humidity (RH) and temperature in ambient environment (OBE, 2002). Compared to RH, the effect of temperature on MC is much weaker (Mirianon et al., 2008, Dietsch et al., 2015a), so the influence of temperature is neglected in this study.

The moisture transfer process will induce MC gradient in the wood sections when the outside RH and temperature are variable or its corresponding EMC is different from the initial MC of timber members. Moreover, the anisotropy of swelling and shrinkage ratio and the existence of MC gradient in wood sections may result in cracks, especially in the transverse directions (Dietsch et al., 2015b, Bonarski et al., 2015). Thus, the study of the MC distribution and change of MC in transverse cross-section with time is essential, which is the basis for the subsequent study of the moisture-induced stress and shrinkage cracks.

Because moisture transport in wood is an unsteady-state process, a diffusion model based on Fick's second law has been developed to describe it (Skaar, 1958). In this model, diffusion coefficient D describes the internal moisture transfer rate in the materials and surface emission coefficient S characterizes the resistance when the water molecules are moving through the material surface. And this model has been accepted by many scholars (Time, 2002, Kadem et al., 2011, Zítek et al., 2015). D and S are influenced by wood type, MC and temperature (Jia and Afzal, 2007). And D in radial direction and tangential direction are assumed to be equal in the following discussion (Fortino et al., 2009). Now, many scholars (Fragiacomo et al.,

Chen, K., Sun, M. and Qiu, H.
Study of Moisture Transfer in Transverse Directions of Timber Members of Anhui Fir.
DOI: 10.5220/0008186901430150
In *The Second International Conference on Materials Chemistry and Environmental Protection (MEEP 2018)*, pages 143-150
ISBN: 978-989-758-360-5
Copyright © 2019 by SCITEPRESS – Science and Technology Publications, Lda. All rights reserved

2011, Qiu, 2015) use the same formulas to calculate D in radial and tangential directions, and S. However, the equation for D is obtained by fitting the experimental results presented in Jönsson's thesis (Jönsson, 2005), and equation for S is from Hoffmeyer's research (Hoffmeyer and Davidson, 1989). Both of above experiments were conducted on Norway spruce. Therefore, it is not accurate to use these formulas directly for different kind wood.

To research the moisture transport in different climate conditions and further mechanical analysis, considering wood is nonlinear material, it is essential to use numerical simulations by the finite element method (FEM). Many authors (Younsi et al., 2007, Fortino et al., 2009, Konopka et al., 2017) used numerical method to analyze moisture transport in wood samples, and DC2D4, a four-node linear heat transfer quadrilateral has been proved to be possible to analyze the process. What's more, the influence of climate on the mechanical properties should also be taken into account for further mechanical analysis, such as crack propagation and capacity of timber member.

The purpose of this study is to evaluate the diffusion coefficient and surface emission coefficient of Anhui fir and use Abaqus heat transfer analysis to simulate the moisture transfer process. In section 2, the analogy between humidity field and temperature field is done to realize the substitution of related parameters, and deriving equations of D and S. In section 3, specific data and phenomenon are acquired by experiment, and specific formulas of D and S will be proposed. In section 4, finite element model is established to realize the moisture transfer process in Abaqus and will be proved valid by comparing the results with experiment.

2 THEORY

2.1 Analogy between Humidity Field and Temperature Field

Wood is assumed to follow Fick's second law for moisture transfer and heat transfer. The moisture transfer in one dimension is modelled as:

$$\frac{\partial u}{\partial t}=\frac{\partial}{\partial x}\left(D\frac{\partial u}{\partial x}\right) \tag{1}$$

where u [%] is the MC of wood, and D [m^2/s] is the coefficient of moisture diffusion.

The differential equation of heat transfer in one dimension can be described as:

$$\frac{\partial T}{\partial t}=\frac{\partial}{\partial x}\left(\frac{\lambda}{c\rho}\frac{\partial T}{\partial x}\right) \tag{2}$$

here T [K] is the temperature, c [J/kg/K] is the specific heat, ρ [kg/m^3] is the wood density and λ [W/m/K] is the thermal conductivity.

The boundary condition of moisture transfer is moisture flux across the surface Γ, which is expressed as:

$$q_{\mathrm{n}}\big|_{\Gamma}=\rho S\left(u_{\mathrm{air}}-u_{\mathrm{surf}}\right) \tag{3}$$

where q_{n} [kg/m^2/s] is the moisture flux across the surface, ρ [kg/m^3] is the wood density in absolute dry condition, S [m/s] is the surface emission coefficient, u_{surf} [%] is the MC of wood surface, and u_{air} [%] is the EMC corresponding to the air RH, defined as equation (4) (Hoffmeyer and Davidson, 1989).

$$u_{\mathrm{air}}=0.01\times\left(\frac{-(T+273.15)\ln(1-RH)}{0.13\left[1-(T+273.15)/647.1\right]^{-6.46}}\right)^{\frac{(T+273.15)^{0.75}}{110}} \tag{4}$$

For temperature field, the boundary condition is expressed as:

$$q_{\mathrm{T}}\big|_{\Gamma}=h\left(T_{\mathrm{air}}-T_{\mathrm{surf}}\right) \tag{5}$$

in which q_{T} [W/m^2] is the heat flux across the surface, h [W/m^2/K] is the film coefficient, T_{surf} [K] is the temperature of wood surface, and T_{air} [K] is the temperature of around air.

When setting density ρ and specific heat c to 1, D and u can replace λ and T respectively by compared formula (1) with (2). Similarly, S can replace h by comparing formula (3) and (5). The analogy of parameters are shown in Table 1.

Table 1: The analogy between parameters of humidity field and temperature field.

Humidity field	Temperature field
u	T
D	λ
S	h
u_{air}	T_{air}
u_{surf}	T_{surf}

2.2 Analysis of Diffusion Coefficient and Surface Emission Coefficient

According to experimental results (referred to experiment section), at certain time t0, the polynomial distribution of MC around the cross-section is obvious, which can be expressed as:

$$u(t_0,r) = m(t_0) + n(t_0)r^2 \tag{6}$$

here m and n are constant when $t = t_0$, and r [mm] is the distance from pith. This distribution result agrees with Jia's conclusion (Jia and Afzal, 2007).

MC changes with time exponentially at certain distance r_0, which is expressed as:

$$u(t,r_0) = A(r_0)\exp(B(r_0)t) + u_{\text{air}} \tag{7}$$

where A and B are constant when $r = r_0$, t [h] is time.

The specimens used are with circular cross-section, based on two-dimension Fick's second law, equation (1) can be described as:

$$\frac{\partial u}{\partial t} = D\left(\frac{\partial^2 u}{\partial r^2} + \frac{\partial u}{r\partial r}\right) \tag{8}$$

From equation (6) and (7), there are

$$\frac{\partial u(t_0,r)}{\partial r} = 2n(t_0)r \tag{9}$$

$$\frac{\partial^2 u(t_0,r)}{\partial r^2} = 2n(t_0) \tag{10}$$

$$\frac{\partial u(t,r_0)}{\partial t} = A(r_0)B(r_0)\exp(B(r_0)t) \tag{11}$$

Substituting equation (9), (10) and (11) to equation (8), there is

$$D = \frac{A(r_0)B(r_0)\exp(B(r_0)t_0)}{4n(t_0)} \tag{12}$$

Equation (3) can also change to:

$$\begin{aligned} q_n &= \rho_0 S\left(-\left.\frac{\partial u}{\partial r}\right|_\Gamma\right)\Delta r = \rho_0(S\Delta r)\left(-\left.\frac{\partial u}{\partial r}\right|_\Gamma\right) \\ &= \rho_0 D\left(-\left.\frac{\partial u}{\partial r}\right|_\Gamma\right) \end{aligned} \tag{13}$$

Therefore, the boundary condition of moisture transfer can also be described as:

$$-\left.\frac{\partial u}{\partial r}\right|_\Gamma = \frac{S}{D}(u_{\text{air}} - u_{\text{surf}}) \tag{14}$$

Substituting equation (9) to equation (14), there is

$$\frac{S}{D} = -\frac{2n(t_0)\,r|_\Gamma}{(u_{\text{air}} - u_{\text{surf}})|_{t_0}} \tag{15}$$

And surface emission coefficient at certain time t_0 can be expressed as:

$$S = -\frac{rA(r)B(r)\exp(B(r)t_0)|_\Gamma}{2(u_{\text{air}} - u_{\text{surf}})|_{t_0}} \tag{16}$$

3 EXPERIMENT

3.1 Materials and Methods

Three specimens [100 (Diameter) × 800 (Length) mm] made of Anhui fir, a kind of Cunninghamia lanceolate were used in this experiment, named CA1, CA2, and CA3 respectively. Wood materials were selected from the same batch, trunks with similar features (size, ring width and so on), and free from decay and insects. All specimens were surface polished and their pith should be in the middle of the cross section. Both longitudinal ends of each specimen were sealed with PE plastic film, ensuring that moisture only exchanged with the outside from transverse directions.

The chamber's temperature was set constant at 40 ℃ to accelerate the procedure during the whole experiment. And RH was set 30% for 10 days. MC distribution of each specimen was measured at 0h, 24h, 48h, 96h, 144h, 192h, and 240h. Before each measurement, the end of each specimen was cut by 10mm with a reciprocating saw to eliminate end interference and then cut off a 20 mm-thick disk in longitudinal direction. After that, remaining part of

SCITEPRESS SCIENCE AND TECHNOLOGY PUBLICATIONS

the specimens were sealed with plastic film again and returned into the chamber. The cutting process is shown in Figure 1.

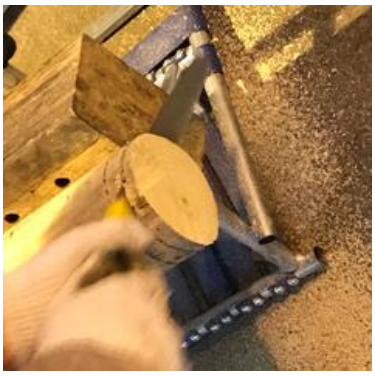

Figure 1: Disk cutting.

Then six small pieces [10 (R) × 10 (T) × 20 (L) mm] were cut symmetrically along the radial direction (as shown in Figure 2). The small pieces were numbered as first circle [small piece 1, 6], second circle [small piece 2, 5], third circle [small piece 3, 4] from outside to inside. Actually, during the experiment, shrinkage cracks occurred and in order to eliminate the influence from cracks, the choice of small pieces were away from cracks.

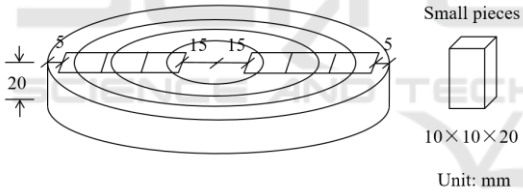

Figure 2: Diagram of cutting small pieces.

MC is calculated by equation (17) (Siau, 1995).

$$u = \frac{m_1 - m_0}{m_0} \times 100\% \qquad (17)$$

where m_1 [g] is the weight tested immediately after cutting and m_0 [g] is the weight in absolute dry condition, dried in oven at 103±2℃.

3.2 Results of Experiment

Figure 3, 4, and 5 show MC distribution versus distance of CA1, CA2, CA3 respectively. It is apparent the MC distribution in transverse cross-section follows the polynomial distribution at any time. Figure 6, 7, and 8 show MC in each circle reduces exponentially versus time.

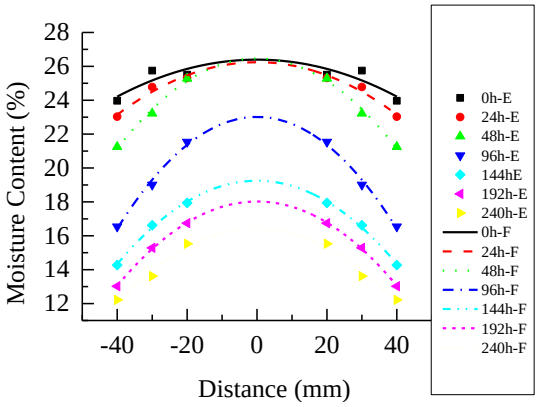

Figure 3: MC distribution of CA1 versus the distance from pith in 0h, 24h, 48h, 96h, 144h, 192h, 240h, dots with letter E are experimental results and lines with letter F are fitting curves based on the results.

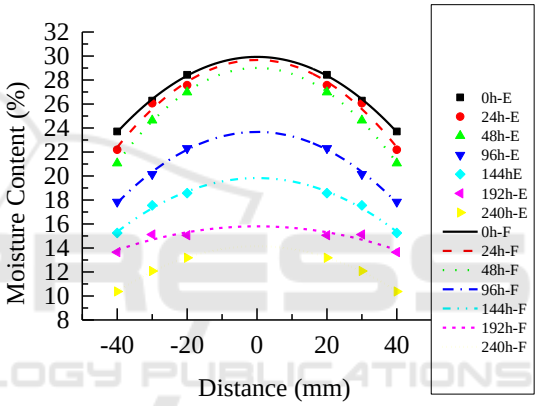

Figure 4: MC distribution of CA2 versus the distance from pith in 0h, 24h, 48h, 96h, 144h, 192h, 240h.

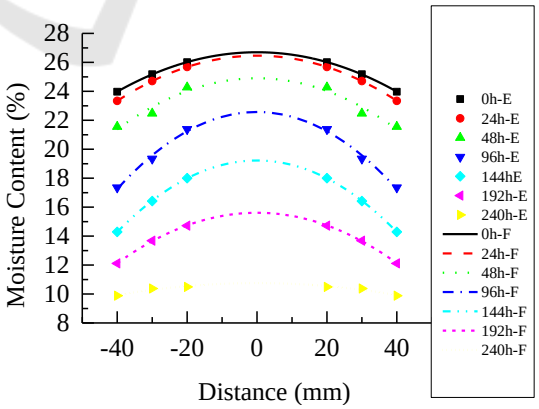

Figure 5: MC distribution of CA3 versus the distance from pith in 0h, 24h, 48h, 96h, 144h, 192h, 240h.

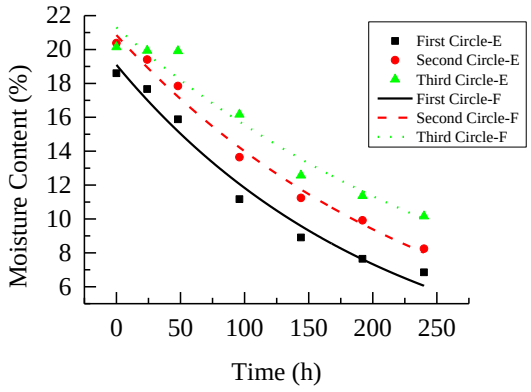

Figure 6: Difference value between MC of each circle in CA1 and EMC corresponding around air versus time (First Circle (r = 40 mm), Second Circle (r = 30 mm) and Third Circle (r = 20 mm)).

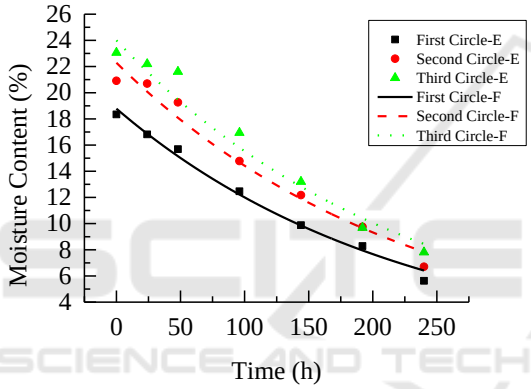

Figure 7: Difference value between MC of each circle in CA2 and EMC corresponding around air versus time.

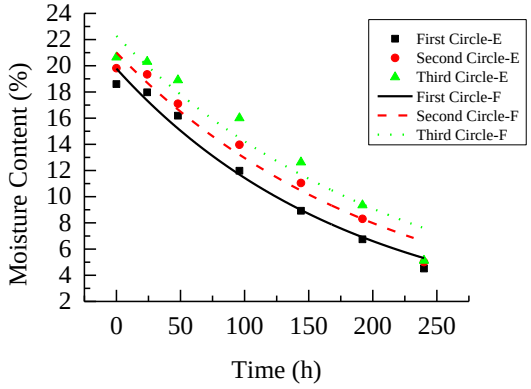

Figure 8: Difference value between MC of each circle in CA3 and EMC corresponding around air versus time.

Table 2 and Table 3 show the fitting results of *m*, *n*, *A*, *B* for each specimen.

Table 2: Values of m and n from fitting curves of each specimen

Specimen	Time/h	Parameter	
		m	*n*/×1E-3
CA1	0	26.40	-1.36
	24	26.25	-1.94
	48	26.46	-3.32
	96	23.02	-4.13
	144	19.25	-3.08
	192	18.02	-3.11
	240	16.41	-2.71
CA2	0	29.93	-3.92
	24	29.67	-4.55
	48	29.01	-4.94
	96	23.67	-3.70
	144	19.83	-2.80
	192	15.80	-1.23
	240	14.15	-2.35
CA3	0	26.70	-1.70
	24	26.46	-1.95
	48	24.90	-2.20
	96	22.57	-3.33
	144	19.22	-3.09
	192	15.61	-2.18
	240	10.75	-0.52

Table 3: Values of A and B from fitting curves of each specimen.

Specimen	Circle	Parameter	
		A	*B*/×1E-3
CA1	1st	18.62	-5.01
	2nd	20.37	-4.15
	3rd	20.81	-3.26
CA2	1st	18.29	-4.68
	2nd	21.80	-4.51
	3rd	24.06	-4.54
CA3	1st	19.30	-5.73
	2nd	20.52	-5.03
	3rd	21.78	-4.64

Figure 9, 10 and 11 show MC changing speed of outside and inner circle of CA1, CA2 and CA3. It is apparent that MC changing speed in every circle is decreasing with time.

In CA1 and CA3, the changing speed of MC in outside circle is quicker than the speed in inner circle at the early period and then becoming slower. The surface of timber member exchanges moisture with ambient air directly, which induces the MC in outside circle changes immediately. Then the moisture in inner circle changed influenced by the existence of MC gradient in different circles, but the response of inner circle is late, which can be defined

as lag. During early period, due to the high MC gradient, the MC changing speed is quick. With time going, MC in outside circle is gradually close to EMC of air, which reduces MC gradient in outside circle and so the MC changing speed becomes much slower at that position, while MC in inner circle keeps changing quickly due to the high overall MC gradient. This indicates that MC gradient has a great influence in MC changing speed, the bigger the MC gradient is, the quicker the speed will be.

But in CA2, the changing rate of MC in inner circle keeps higher than that in outside circle. It can be found from Figure 4 that the initial overall MC gradient of CA2 is much larger than others, so the MC in inner circle changes quicker than the outside at the beginning. Apart from that, although the ring width in each specimens are similar, the ring width of CA2 is a little bit narrower than the others, which means that the density of CA2 should also be larger. With high density, it can be easier for CA2 to translate moisture in inner circle, which is perhaps the reason of such different speed happened in CA2.

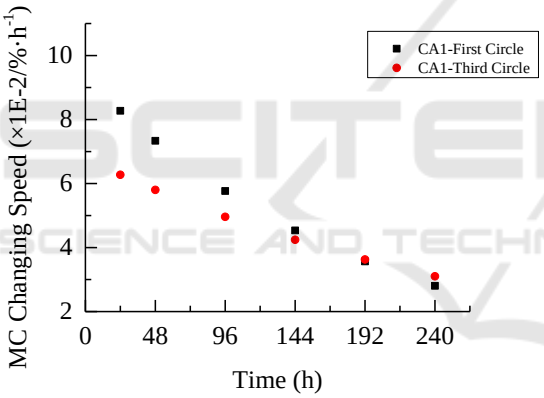

Figure 9: Comparing MC changing speed of inner and outside circle in CA1.

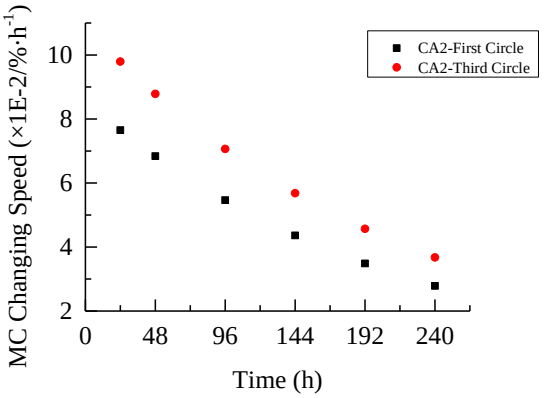

Figure 10: Comparing MC changing speed of inner and outside circle in CA2.

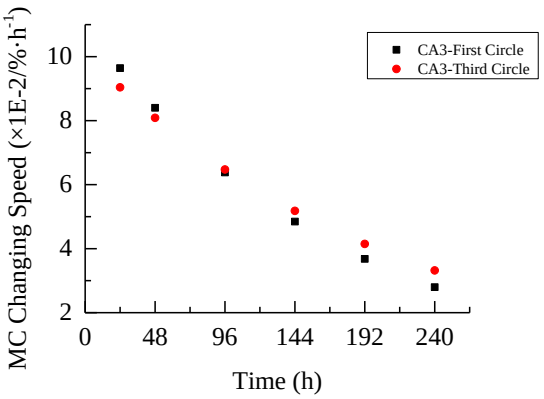

Figure 11: Comparing MC changing speed of inner and outside circle in CA3.

Based on Table 2 and Table 3, D and S can be calculated by equation (12), (16). And the fitting curve of D versus MC is shown in Figure 12. The relationship between diffusion coefficient and MC at 40 ℃ can be expresses as below:

$$D_R(u) = D_T(u) = 2.56 \times e^{2.66u} (\mathrm{mm}^2/\mathrm{h}) \quad (18)$$

where DR is diffusion coefficient in radial direction and DT is diffusion coefficient in tangential direction.

The value of S/D is approximately constant at 0.05/mm during the whole drying stage, so surface emission coefficient of CA can be expressed as:

$$S = 0.128 \times e^{2.66u} (\mathrm{mm/h}) \quad (19)$$

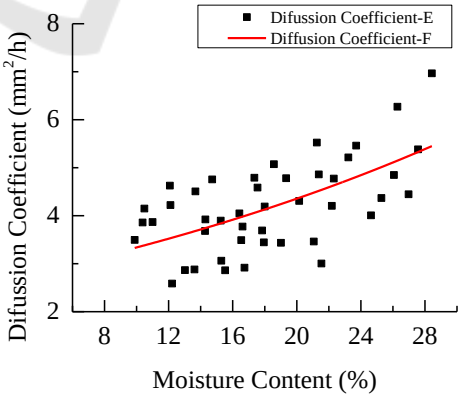

Figure 12: Diffusion coefficient data and fitting curve versus MC.

4 NUMERICAL ANALYSIS

4.1 Finite Element Model (FEM)

According to the corresponding relationship shown in table 1, DC2D4 (a 4 node-linear heat transfer quadrilateral) was used in Abaqus to allow the calculation of moisture transfer. All the geometric and humidity field parameters set in FEM were the same as experiment.

4.2 Results and Discussion

Figure 13, 14, and 15 compare MC of different circles between experimental results and FEM results, and plot MC in pith and surface calculated by Abaqus as well. There is a good agreement between experimental results and FEM results, and the average relative error is less than 5%, which proves the validity of this FEM and the correctness of equation (18) and (19).

The FEM results show that the MC gradient between surface and first circle increases during early period, and then decreases, which is the same trend as experiment shows. Additionally, the biggest MC gradient occurs in out circle as well. This explains the initial occurrence of shrinkage crack in out circle of timber members, and the quick response of outer circle to the environment.

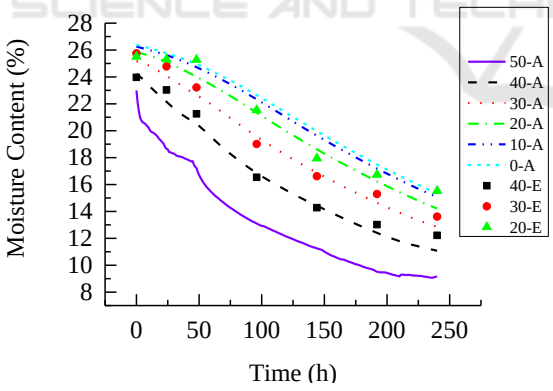

Figure 13: Experimental results versus numerical FEM calculations of CA1.

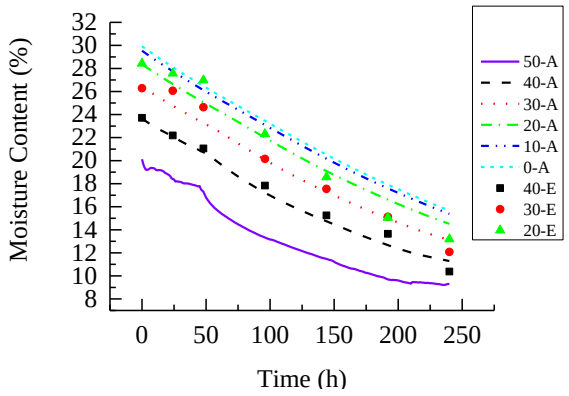

Figure 14: Experimental results versus numerical FEM calculations of CA2.

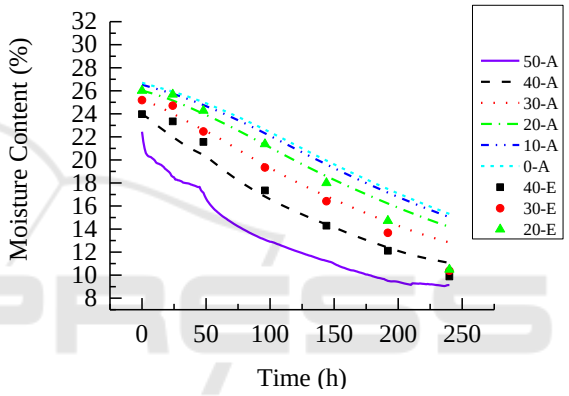

Figure 15: Experimental results versus numerical FEM calculations of CA3.

5 CONCLUSIONS

This paper describes a study of moisture transfer perpendicular to grain in timber members made of Anhui fir. Three cylindrical specimens were used to test the essential parameters for calculating diffusion coefficient and surface emission coefficient. Then a Finite model method was used to analyse the moisture transfer process. And the FEM results agree well with the experiment. Fick's second law of moisture transfer in wood was used in all theoretical derivation and numerical simulations. The primary investigated results are listed below:

(1) The type of wood cannot be ignored when calculating diffusion coefficient and surface emission coefficient. It is not accurate to calculate two coefficient by formula from other wood. And authors analysed the D and S suitable for Anhui fir.

(2) MC in transverse cross-section of Anhui fir shows polynomial distribution at any time, and changes exponentially with time in drying environment.

(3) MC gradient has a great influence in MC changing speed, the larger the MC gradient is, the quicker the speed will be.

(4) The method of substituting corresponding variables in heat transfer in Abaqus to simulate moisture transfer is valid.

Further research related to moisture transfer of timber members in changing climate is still required. Different initial MC distribution should also be taken into consideration. Moreover, moisture-induced stress and shrinkage cracks of timber members are also essential research aspects for timber buildings.

ACKNOWLEDGEMENTS

The authors would like to express their gratitude to the whole staff in Key laboratory of concrete and pre-stressed concrete structure of Ministry of Education, Southeast University and Laboratory of Modern Wood Structure, Nanjing University of Technology for their technical support. And this study was funded by the Thirteenth Five-Year National Key Research and Development Program (2017YFC0703503).

REFERENCES

Bonarski, J. T., Kifetew, G. & Olek, W. 2015, "Effects of cell wall ultrastructure on the transverse shrinkage anisotropy of Scots pine wood", Holzforschung, Vol. 69 No. 4, pp. 501-507.

Dietsch, P., Gamper, A., Merk, M. & Winter, S. 2015a, "Monitoring building climate and timber moisture gradient in large-span timber structures", Journal of Civil Structural Health Monitoring, Vol. 5 No. 2, pp. 153-165.

Dietsch, P., Franke, S., Franke, B., Gamper, A. & Winter, S. 2015b, "Methods to determine wood moisture content and their applicability in monitoring concepts", Journal of Civil Structural Health Monitoring, Vol. 5 No. 2, pp. 115-127.

Fragiacomo, M., Fortino, S., Tononi, D., Usardi, I. & Toratti, T. 2011, "Moisture-induced stresses perpendicular to grain in cross-sections of timber members exposed to different climates", Engineering Structures, Vol. 33 No. 11, pp. 3071-3078.

Fortino, S., Mirianon, F. & Toratti, T. 2009, "A 3D moisture-stress FEM analysis for time dependent problems in timber structures", Mechanics of time-dependent materials, Vol. 13 No. 4, pp. 333.

Hoyle Jr, R. J., Itani, R. Y. & Eckard, J. J. 2007, "Creep of Douglas Fir Beams Due to Cyclic Humidity Fluctuations", Wood and Fiber Science, Vol. 18 No. 3, pp. 490-497.

Hoffmeyer, P. & Davidson, R. W. 1989, "Mechano-sorptive creep mechanism of wood in compression and bending", Wood Science and Technology, Vol. 23 No. 3, pp. 215-227.

Jia, D. & Afzal, M. T. 2007, "Modeling of moisture diffusion in microwave drying of hardwood", Drying technology, Vol. 25 No. 3, pp. 449-454.

Jönsson, J. 2005, "Moisture induced stresses in timber structures". Lund, Lund Institute of Technology.

Kadem, S., Lachemet, A., Younsi, R. & Kocaefe, D. 2011, "3d-Transient modeling of heat and mass transfer during heat treatment of wood", International Communications in Heat and Mass Transfer, Vol. 38 No. 6, pp. 717-722.

Konopka, D., Gebhardt, C. & Kaliske, M. 2017, "Numerical modelling of wooden structures", Journal of Cultural Heritage, Vol. 27, pp. 93-S102.

Mirianon, F., Fortino, S. & Toratti, T. 2008, "A method to model wood by using ABAQUS finite element software", Fire Safety Journal, Vol. 43.

Obe, J. D. 2002, Timber: its nature and behaviour, CRC Press.

Qiu, L. 2015, "Performance of curved glulam beams under load and moisture variations". Harbin, Harbin Institute of Technology.

Ranta-Maunus, A. 2003, "Effects of climate and climate variations on strength", Timber engineering, 153-167.

Skaar, C. 1958, "Moisture movement in beech below the fiber saturation point", Forest Products Journal, No. 8, pp. 352-357.

Siau, J. F. 1995, Wood: Influence of moisture on physical properties, Dept. of Wood Science and Forest Products, Virginia Polytechnic Institute and State University.

Toratti, T. 1994, "Creep of timber beams in a variable environment". Espoo, Teknillinen korkeakoulu.

Time, B. 2002, "Studies on hygroscopic moisture transport in Norway spruce (Picea abies) Part 1: Sorption measurements of spruce exposed to cyclic step changes in relative humidity", Holz als Roh-und Werkstoff, Vol. 60 No. 4, pp. 271-276.

Younsi, R., Kocaefe, D., Poncsak, S. & Kocaefe, Y. 2007, "Computational modelling of heat and mass transfer during the high-temperature heat treatment of wood", Applied Thermal Engineering, Vol. 27 No. 8-9, pp. 1424-1431.

Zítek, P., Vyhlídal, T., Fišer, J., Tornari, V., Bernikola, E. & Tsigarida, N. 2015, "Diffusion-model-based risk assessment of moisture originated wood deterioration in historic buildings", Building and Environment, Vol. 94, 218-230.